Proceedings World Geothermal Congress 2020+1
Reykjavik, Iceland, April - October 2021

Particle Transport in Fractures: A Common Problem in Enhanced Geothermal Systems and Hydraulic Fractures

Saeed Salimzadeh[1], James Kear[1], and Hamid M. Nick[2]

[1]Commonwealth Scientific and Industrial Research Organisation, Clayton, Australia

[2]Danish Hydrocarbon Research and Technology Centre, Technical University of Denmark, Lyngby, Denmark

saeed.salimzadeh@csiro.au

Keywords: Proppant transport, density-driven flow, gravity settlement, hydraulic fracturing

ABSTRACT

Particle transport within fractures is a common problem in hydraulic fractures and in Enhanced Geothermal Systems (EGS). In hydraulic fractures, proppant is used to keep the fractures open after the hydraulic pressure is released. Proppant concentration alters the fracturing fluid properties including dynamic viscosity and density, affecting the hydraulic fracture shape and direction especially in vertical fractures. The distribution of proppant particles over the induced fracture is crucial in maintaining the hydraulic conductivity of a fracture. In this work, a three-dimensional finite element model has been developed to simulate particle transport in fractures. Hydraulic fractures are modelled discretely as surfaces in a 3D matrix. Hydraulic fracture propagation is defined within the Linear Elastic Fracture Mechanics (LEFM) framework. Both proppant settlement and density flow are considered for movement of proppant particles in propagating vertical hydraulic fractures. The model also accounts for depth-increasing in-situ stresses. Results show that the downward movement of proppant encourages downward hydraulic fracture growth, while the depth-increasing in-situ stresses encourage the hydraulic fractures to grow upward.

1. INTRODUCTION

Hydraulic fracture stimulation has been extensively used to improve reservoir performance in hydrocarbon (Economides and Nolte 2000) as well as geothermal reservoirs (McClure and Horne 2014), and for preconditioning the rock masses in underground mines (Jeffrey and Mills 2000). Accurate modelling of hydraulic fracture geometry in the presence of stress gradients, proppant injection, and rock layering is a fundamental requirement for reliable treatment design. In Enhanced Geothermal Systems (EGS), the economic success of heat production relies on successfully creating fractures in otherwise impermeable rocks and maintaining the opening and hydraulic conductivity of the created fractures conductive during the lifetime of the EGS. Fractures in EGS suffer from decaying permeability due to dissolution of asperities under in-situ stresses (Detwiler 2008; Salimzadeh and Nick 2019).

In hydraulic fracturing stimulation, proppant is added to the hydraulic fracturing fluids so that the created fracture remains open and maintain a conductive channel or network to the wellbore (McLennan, Green, and Bai 2008). The presence and distribution of proppant have a crucial role in retaining fracture permeability (Gu et al. 2014), and therefore fracture contribution to overall production (Cipolla et al. 2008). Thus, modelling the hydraulic fracture propagation considering only a viscous fluid is not optimal, since the proppant concentration alters the properties of the hydraulic fracturing fluid, i.e. slurry. A first-order correction to the viscosity of dilute suspensions was first introduced by Einstein. Later, a second-order correction was made by Batchelor and Green (Batchelor and Green 1972). The hydraulic fracturing fluid (slurry) is commonly modelled as a Newtonian fluid, with viscosity dependence on proppant concentration. The proppant distribution across the fracture is assumed to be uniform and only the slip velocity due to gravity is considered (Adachi et al. 2007).

Recently, the problem of proppant transport in hydraulic fractures has attracted a great deal of attention in the hydraulic fracturing community. Dontsov and Peirce presented a model for the steady flow of a Newtonian fluid mixed with spherical particles in a channel for the purpose of modelling proppant transport with gravitational settling in hydraulic fractures (Dontsov and Peirce 2014). Wang and Elsworth presented a 2D model for the evolution of the residual aperture profile and conductivity of hydraulic fractures partially/fully filled with proppant packs (Wang and Elsworth 2018). Shi et al. presented a XFEM-based model to calculate conductivity of a propped hydraulic fracture considering proppant transport, embedment and crushing (Shi et al. 2018). Vahab and Khalili presented a 2D XFEM model for the problem of graded, nonuniform proppant injection and settlement (Vahab and Khalili 2018).

The problem of proppant distribution and settling becomes even more significant in vertical fractures. In addition to the proppant settlement, the higher concentration of proppant increases the density of the hydraulic fracturing fluid (slurry), resulting in a density-driven downward flow. Local stresses on the other hand increase with depth resulting in depth-increasing effective stresses, preventing the downward growth of hydraulic fractures (Salimzadeh et al. 2019). In this study, a fully coupled three-dimensional finite element model is presented to investigate the propagation of hydraulic fractures with proppant injection. Both gravity settlement of proppant and density-driven slurry flow are considered. The depth-increasing in-situ stresses are applied for vertical hydraulic fractures and, the shape and propagation direction of hydraulic fractures are investigated.

2. COMPUTATIONAL MODEL

In the present approach, hydraulic fractures are modelled as surface discontinuities in the three-dimensional matrix (Paluszny and Zimmerman 2013). The deformation model is expressed satisfying the condition of equilibrium on a representative elementary volume (REV) of the porous medium. Fracture surfaces are not traction-free in the present model, and hydraulic loading are applied

on the fracture walls. Assuming negligible shear tractions exerted from the fluid on the fracture surfaces, the fluid pressure is applied only in the normal direction to the fracture wall. The differential equation describing the deformation field for a representative elementary volume (REV) of fractured rock is given by

$$\mathrm{div}(\mathbf{D}\boldsymbol{\varepsilon}) + \mathbf{F} - p_f \mathbf{n}_c \delta(\mathbf{x} - \mathbf{x}_c) = 0 \tag{1}$$

where, $\mathbf{D}$ is the drained stiffness matrix, $\boldsymbol{\varepsilon} = \frac{1}{2}(\nabla\mathbf{u} + \nabla\mathbf{u}^T)$ is the strain tensor in the porous medium, $\mathbf{u}$ denotes the displacement vector in the porous medium, $\mathbf{F}$ is the body force per unit volume, p_f is the fluid pressure, δ is Dirac delta, and $\mathbf{x}_c$ represents the position of the fracture. The flow through fracture is assumed to be laminar

$$\mathrm{div}\left[\frac{{a_f}^3}{12\mu_{sl}}(\nabla p_f + \rho_{sl}\mathbf{g})\right] = a_f c_f \frac{\partial p_f}{\partial t} + \frac{\partial a_f}{\partial t} \tag{2}$$

where, a_f is the fracture aperture, μ_{sl} is the slurry viscosity, $\rho_{sl} = (1 - C_p)\rho_f + C_p\rho_p$ is the density of slurry, C_p is the volumetric concentration of proppant in slurry, ρ_f is the density of fluid, ρ_p is the density of proppant particles, $\mathbf{g}$ is the gravitational vector, and c_f is the fluid compressibility. Note that the term $\partial a_f/\partial t = \partial(\mathbf{u}^+ - \mathbf{u}^-).\mathbf{n}_c/\partial t$ provides direct coupling between the displacement field and the fracture flow field, which is symmetric to the fracture pressure loading term, $p_f\mathbf{n}_C$ in Eq. 1. $\mathbf{u}^+$ and $\mathbf{u}^-$ are the displacements of the two opposing faces of the fracture. The rheology of the slurry is affected by the proppant concentration, which can be described by the following expression (Barree and Conway 1995)

$$\mu_{sl} = \mu_f \left(1 - \frac{C_p}{C_0}\right)^{-m} \tag{3}$$

where, μ_f is the fluid viscosity without proppant, $C_0 = 0.6$ is the maximum attainable proppant concentration, and $m = 1.05$ is a model parameter. Effective values of C_0 range from 0.59 to 0.64 and m ranges from 1 to 3, depending on the type of proppant and hydraulic fracturing fluid (Barree and Conway 1995; Adachi et al. 2007). The governing equation for the proppant transport through the fracture can be written as

$$\mathrm{div}\left[a_f D_p \nabla(\rho_p C_p)\right] = \frac{\partial(a_f \rho_p C_p)}{\partial t} + \nabla.\left(a_f \rho_p \mathbf{v}_p C_p\right) \tag{4}$$

where, D_p is the proppant dispersion coefficient and $\mathbf{v}_p$ is the proppant velocity in slurry. Velocity of proppant differs from the velocity of slurry due to slippage of proppant particles during gravitational settling and blocking. To effectively prevent the proppant from moving into the narrow regions, the proppant flux needs to be multiplied by a 'blocking' function, to account for the proppant stalling in the narrow fracture regions. The blocking function B_{a_f} is defined as (Dontsov and Peirce 2014)

$$B_{a_f} = \frac{1}{2}H\left(\frac{a_f}{d_p} - N\right)H\left(\frac{a_c - a_f}{d_p}\right)\left[1 + \cos\left(\pi\frac{a_c - a_f}{d_p}\right)\right] + H\left(\frac{a_f - a_c}{d_p}\right) \tag{5}$$

where, H denotes the Heaviside step function, N represents number of proppant particles passing through a section, $a_c = d_p(N + 1)$ is the critical aperture at which the blocking starts to occur, and d_p is the proppant particle diameter. Single-particle gravitational settling velocity in an unbounded medium in Stokes regime (low Reynolds number regime) can be expressed as (Barree and Conway 1995)

$$\mathbf{v}_t = \frac{{d_p}^2(\rho_p - \rho_f)}{18\mu_f}\mathbf{g} \tag{6}$$

The Stokes' equation is limited to a single particle in an infinite fluid mass falling under conditions of laminar flow. In general, Stokes' law is valid for viscous Newtonian fluids or for small particle sizes (Barree and Conway 1995). The presence of other particles will change the drag force exerted on each particle. The motion of other particles creates a "return flow" of carrying fluid, and the single-particle settling velocity should be corrected for the effect of proppant concentration. The correction factor is defined as (Goview and Aziz 1972)

$$f_{C_p} = e^{-5.9C_p} \tag{7}$$

Thus, the proppant velocity $\mathbf{v}_p$ is computed from the slurry velocity $\mathbf{v}_{sl}$, subject to settling and blocking according to

$$\mathbf{v}_p = B_{a_f}\left(\mathbf{v}_{sl} + f_{C_p}\mathbf{v}_t\right) \tag{8}$$

The governing equations are solved numerically using the finite element method. Spatial and temporal discretization are accomplished using the Galerkin method and finite difference techniques, respectively. Displacements (three displacements for three dimensions), hydraulic fracturing fluid (slurry) pressure and concentration are defined as the primary variables. Quadratic unstructured elements are used for spatial discretization of surfaces (quadratic triangles) and volumes (quadratic tetrahedra). The triangles on two opposite surfaces of a fracture are matched with each other, but do not share nodes, and duplicate nodes are defined for two sides of a fracture. The triangles are matched with faces of the tetrahedra connected to the fractures, and they share the same nodes. Flow through deforming fracture is a highly nonlinear problem, thus a Picard iteration procedure is adopted to reach the correct solution within acceptable tolerance. More details on the computational model can be found in (S. Salimzadeh and Nick 2019; Usui et al. 2017; S. Salimzadeh, Paluszny, and Zimmerman 2018). The discretized equations are implemented in the Complex Systems Modelling Platform (CSMP, also known as CSP, (Matthäi, Geiger, and Roberts 2001)), an object-oriented application program interface (API), for the simulation of complex geological processes and their interactions. The set of linear algebraic equations are solved with the

algebraic multigrid method for systems, SAMG (Stüben 2001). Within the framework of Linear Elastic Fracture Mechanics (LEFM), the stress intensity factors (SIFs) for three modes of fracture opening are computed using the displacement correlation method (DC method, (Paluszny and Zimmerman 2013)). The DC method is computationally cheap and is able to yield very good approximations of the SIFs (Kuna 2013). The crack grows when the equivalent stress intensity factor K_{eq} (Schöllmann et al. 2002) overcomes the material toughness (k_{ic}). At every timestep, the SIFs and growth computations are performed at forty locations along the fracture front (fracture tips). If the equivalent SIF reaches the material toughness in at least one fracture tip, the propagation triggers and all the fracture tips are advanced proportionally to the equivalent SIF value at each tip. Then, the fracture geometry is updated, the mesh is regenerated, and the step is recalculated for the new geometry.

2. SIMULATION RESULTS

The numerical finite element model has been validated extensively against analytical, experimental and numerical results in the literature (S. Salimzadeh, Paluszny, and Zimmerman 2016; S. Salimzadeh et al. 2019; Saeed Salimzadeh et al. 2019; S. Salimzadeh and Nick 2019; Peters et al. 2018). In this section, the geometry of a vertical hydraulic fracture induced from a horizontal well under varying in-situ stresses and proppant concentration is investigated. An injection of water with flow rate 0.015 m^3/s for a duration of 5000 seconds is considered. The material properties are given in Table 1.

Four cases are considered: In case I, no proppant is injected, and the vertical gradient of in-situ stress is set to 10 kPa/m, equal to hydrostatic pressure gradient (the gravitational acceleration is set to g = 10 m^2/s). In case II the proppant is added to case I. Case III is similar to case I but with a vertical in-situ stress gradient of 20 kPa/m (lithostatic pressure gradient). Finally, in case IV, the proppant is added to case III. For cases with proppant injection, after 200 seconds of "pad" (water without proppant), a volumetric concentration of 0.3 of proppant is added to the water.

Table 1: Material properties used for simulations

	Case I	Case II	Case III	Case IV
Injection rate (m^3/s)	0.015	0.015	0.015	0.015
Water density (kg/m^3)	1000	1000	1000	1000
Water viscosity (Pa s)	0.001	0.001	0.001	0.001
Young's modulus (GPa)	20	20	20	20
Poisson's ratio	0.25	0.25	0.25	0.25
Fracture toughness (MPa $m^{0.5}$)	1.0	1.0	1.0	1.0
In-situ stress gradient (kPa/m)	10	10	25	25
Proppant concentration at injection	0	0.3	0	0.3
Proppant density (kg/m^3)	-	2500	-	2500

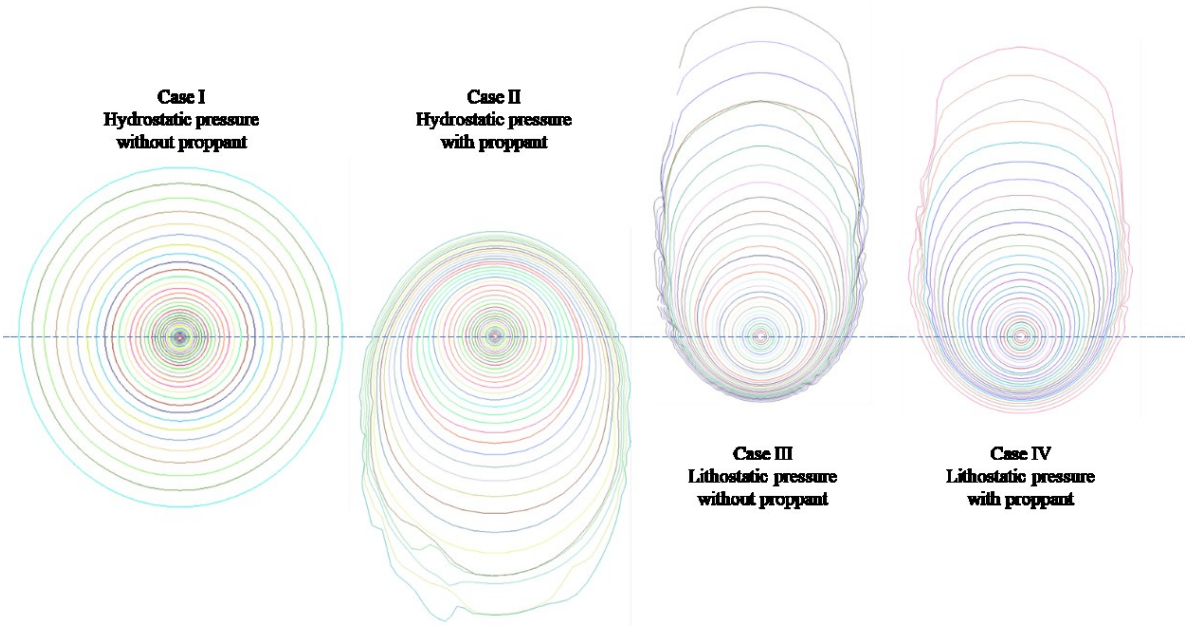

Figure 1: The geometry of induced fractures at each propagation step for different cases. The dashed line shows the depth of initial perforation (horizontal well).

The geometry of induced fractures for four cases are shown in Figure 1. In case I, a round radial hydraulic fracture is created around the injection point. This is due to the equilibrium between hydrostatic pressure of water (without proppant) and the applied in-situ stresses. In case II, the fracture initially grows in radial shape during the injection of pad (water without proppant), but as soon as the proppant enters the fracture, the density of slurry increases, the equilibrium between the hydrostatic pressure inside the fracture and the applied stresses is violated and thus the fracture preferably grows downward. In case III, the higher lithostatic stress gradient pushes the fracture to grow upward, where the applied stresses are smaller than the slurry pressure. The propagation is dominantly upward with little downward or sideward propagation. In case IV, the overall growth of the fracture is still upward, however, the presence of proppant encourages the downward and sideward growth of the fracture compared to case III.

The distribution of proppant concentration, fracture aperture, and slurry pressure in the hydraulic fracture in case II and IV are shown in Figure 2 and Figure 3, respectively. Downward movement of proppant from the injection point due to settlement and density-driven flow is clearly observed in case II. The proppant concentration increases the slurry viscosity and density; thus, the slurry pressure increases, resulting in an increase in the fracture aperture towards the bottom of fracture. However, the blocking function prevents the proppant of reaching to the fracture tips. In case IV, the higher in-situ gradient forces the fracture to grow upward from the injection point. The proppant remains mainly in the bottom part of the fracture, and aperture increases in both top and bottom parts of fracture due to lower stress in the former and higher pressure in the latter.

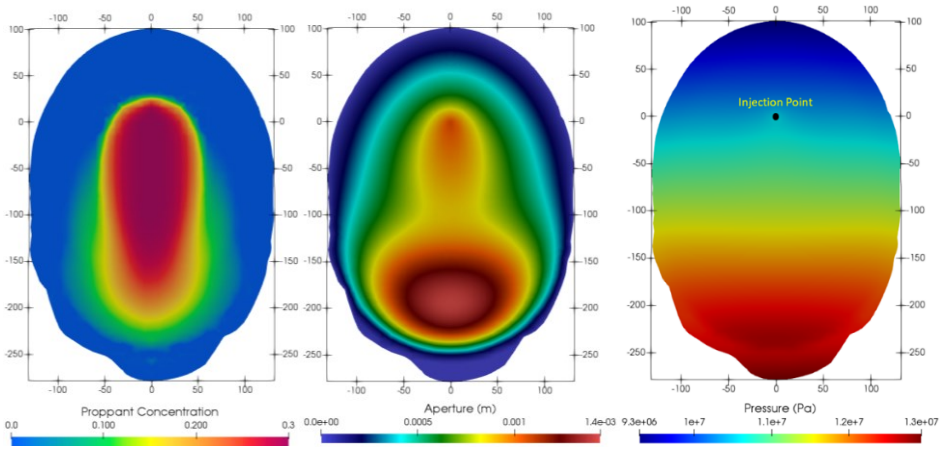

Figure 2: Proppant concentration, fracture aperture and slurry pressure distribution for case II with hydrostatic in-situ stress (stress gradient of 10 kPa/m).

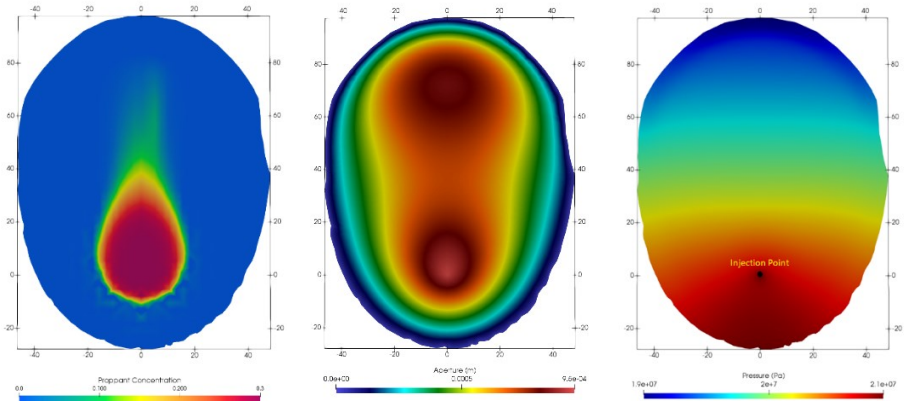

Figure 3: Proppant concentration, fracture aperture and slurry pressure distribution for case IV with lithostatic in-situ stress (stress gradient of 20 kPa/m).

3. CONCLUSIONS

The simulation results show that gravity has a significant effect on the shape and direction of hydraulic fractures. The fracture shape can be far from a round shape predicted by simple analytical solutions. Gravity triggers competing effects: while it induces proppant settlement and downward density-driven flow, resulting in downward growth of hydraulic fractures, simultaneously, gravity increases the lithostatic in-situ pressure, encouraging upwards growth of hydraulic fractures.

ACKNOWLEDGEMENT

Part of this study was developed during Saeed Salimzadeh's visit to the Danish Hydrocarbon Research and Technology Centre (DHRTC) in May 2019. Author Saeed Salimzadeh would like to thank DHRTC for providing the financial support for the visit, and thanks the Commonwealth Scientific and Industrial Research Organisation (CSIRO) for approving the visit and collaboration.

REFERENCES

Adachi, J., E. Siebrits, A. Peirce, and J. Desroches. 2007. "Computer Simulation of Hydraulic Fractures." *International Journal of Rock Mechanics and Mining Sciences* 44: 739–57. https://doi.org/10.1016/j.ijrmms.2006.11.006.

Barree, R.D., and M.W. Conway. 1995. "Experimental and Numerical Modeling of Convective Proppant Transport." *Journal of Petroleum Technology* 47 (03): 216–22. https://doi.org/10.2118/28564-pa.

Batchelor, G. K., and J. T. Green. 1972. "Of Spherical Particles To Order C2." *Journal of Fluid Mechanics* 56 (3): 401–27. http://sor.scitation.org/doi/10.1122/1.548848.

Cipolla, C L, N R Warpinski, M J Mayerhofer, E P Lolon, Pinnacle Technologies, and M C Vincent. 2008. "SPE 115769 The Relationship Between Fracture Complexity , Reservoir Properties , and Fracture Treatment Design." *Network*, 1–25.

Detwiler, Russell L. 2008. "Experimental Observations of Deformation Caused by Mineral Dissolution in Variable-Aperture Fractures." *Journal of Geophysical Research: Solid Earth* 113: B08202. https://doi.org/10.1029/2008JB005697.

Dontsov, E. V., and A. P. Peirce. 2014. "Slurry Flow, Gravitational Settling and a Proppant Transport Model for Hydraulic Fractures." *Journal of Fluid Mechanics* 760 (1): 567–90. https://doi.org/10.1017/jfm.2014.606.

Economides, Michael J., and Kenneth G. Nolte. 2000. "Reservoir Stimulation." New York.

Goview, G.W., and K. Aziz. 1972. *The Flow of Complex Mixtures in Pipes*. Malabar, FL: Robert E. Krieger Publishing Co.

Gu, Ming, Pandurang Kulkarni, Mehdi Rafiee, and Endre Ivarrud. 2014. "Understanding the Optimum Fracture Conductivity for Naturally Fractured."

Jeffrey, R G, and K W Mills. 2000. "Hydraulic Fracturing Applied to Inducing Longwall Coal Mine Goaf Falls." In *Pacific Rocks 2000*, 423–30. Rotterdam.

Kuna, Meinhard. 2013. *Finite Elements in Fracture Mechanics - Theory - Numerics - Applications*. Springer Netherlands. https://doi.org/10.1007/978-94-007-6680-8.

Matthäi, S.K., S. Geiger, and S.G. Roberts. 2001. "Complex Systems Platform: CSP3D3.0 User's Guide." https://doi.org/10.3929/ethz-b-000251651.

McClure, Mark W., and Roland N. Horne. 2014. "An Investigation of Stimulation Mechanisms in Enhanced Geothermal Systems." *International Journal of Rock Mechanics and Mining Sciences* 72: 242–60. https://doi.org/10.1016/j.ijrmms.2014.07.011.

McLennan, J. D., S.J. Green, and M. Bai. 2008. "Proppant Placement During Tight Gas Shale Stimulation: Literature Review And Speculation." In *42nd US Rock Mechanics Symposium*. American Rock Mechanics Association.

Paluszny, Adriana, and Robert W. Zimmerman. 2013. "Numerical Fracture Growth Modeling Using Smooth Surface Geometric Deformation." *Engineering Fracture Mechanics* 108: 19–36. https://doi.org/10.1016/j.engfracmech.2013.04.012.

Peters, Elisabeth, Guido Blöcher, Saeed Salimzadeh, Paul J.P. Egberts, and Mauro Cacace. 2018. "Modelling of Multi-Lateral Well Geometries for Geothermal Applications." *Advances in Geosciences* 45: 209–15. https://doi.org/10.5194/adgeo-45-209-2018.

Salimzadeh, S., M. Grandahl, M. Medetbekova, and H.M. Nick. 2019. "A Novel Radial Jet Drilling Stimulation Technique for Enhancing Heat Recovery from Fractured Geothermal Reservoirs." *Renewable Energy*, February. https://doi.org/10.1016/J.RENENE.2019.02.073.

Salimzadeh, S., and H. M. Nick. 2019. "A Coupled Model for Reactive Flow through Deformable Fractures in Enhanced Geothermal Systems." *Geothermics* 81 (October 2018): 88–100. https://doi.org/10.1016/j.geothermics.2019.04.010.

Salimzadeh, S., A. Paluszny, and R.W. Zimmerman. 2016. "Thermal Effects during Hydraulic Fracturing in Low-Permeability Brittle Rocks." In *50th US Rock Mechanics / Geomechanics Symposium 2016*. Vol. 1.

Salimzadeh, S., A. Paluszny, and R.W. Zimmerman. 2018. "Effect of Cold CO<inf>2</Inf>injection on Fracture Apertures and Growth." *International Journal of Greenhouse Gas Control* 74. https://doi.org/10.1016/j.ijggc.2018.04.013.

Salimzadeh, S., Eirik D. Hagerup, Teeratorn Kadeethum, and Hamidreza M. Nick. 2019. "The Effect of Stress Distribution on the Shape and Direction of Hydraulic Fractures in Layered Media." *Engineering Fracture Mechanics* 215: 151–63. https://doi.org/10.1016/j.engfracmech.2019.04.041.

Schöllmann, Matthias, Hans A. Richard, Gunter Kullmer, and Markus Fulland. 2002. "A New Criterion for the Prediction of Crack Development in Multiaxially Loaded Structures." *International Journal of Fracture* 117: 129–41. https://doi.org/10.1023/A:1020980311611.

Shi, Fang, XiaoLong Wang, Chuang Liu, He Liu, and HengAn Wu. 2018. "An XFEM-Based Numerical Model to Calculate Conductivity of Propped Fracture Considering Proppant Transport, Embedment and Crushing." *Journal of Petroleum Science and Engineering* 167 (August): 615–26. https://doi.org/10.1016/J.PETROL.2018.04.042.

Stüben, K. 2001. "A Review of Algebraic Multigrid." *Journal of Computational and Applied Mathematics* 128 (1–2): 281–309. https://doi.org/10.1016/S0377-0427(00)00516-1.

Usui, T., S. Salimzadeh, A. Paluszny, and R.W. Zimmerman. 2017. "Effect of Poroelasticity on Hydraulic Fracture Interactions." In *Poromechanics 2017 - Proceedings of the 6th Biot Conference on Poromechanics*. https://doi.org/10.1061/9780784480779.249.

Vahab, M., and N. Khalili. 2018. "An X-FEM Formulation for the Optimized Graded Proppant Injection into Hydro-Fractures Within

Saturated Porous Media." *Transport in Porous Media* 121 (2): 289–314. https://doi.org/10.1007/s11242-017-0959-0.

Wang, Jiehao, and Derek Elsworth. 2018. "Role of Proppant Distribution on the Evolution of Hydraulic Fracture Conductivity." *Journal of Petroleum Science and Engineering*. https://doi.org/10.1016/j.petrol.2018.03.040.